

LPT Orsay 00-72  
August 2000

## ON THE MICROSCOPIC DYNAMICS OF DCC FORMATION

Julien SERREAU

LPT, Bâtiment 210, Université Paris-Sud, 91405 Orsay, France<sup>1</sup>

### Abstract

The dynamics of the pion field after a quench is studied in the framework of the linear sigma model. Our aim is to determine to what extent the amplified pion field resembles the DCC picture originally proposed in the early '90s. We present the result of a computer experiment where, among other things, we study in detail the correlation between isospin orientations of the distinct modes of the field. We show that this correlation is absent. In a sense, the distinct modes behave as distinct DCCs. The implications of this observation are discussed.

## 1 Introduction

A disoriented chiral condensate (DCC) is a medium where “the quark condensate,  $\langle 0|q_L\bar{q}_R|0\rangle$ , is chirally rotated from its usual orientation in isospin space” [1]. This hypothetical object has attracted the attention of many physicists in the last decade and is still a topic of intense theoretical as well as experimental investigations (see reviews [2] and also [3]).

One imagines a rapidly expanding fireball, produced in a high energy hadronic or nuclear collision, whose interior is separated from the outside vacuum by a thin, hot shell of hadronic debris. The quark condensate inside the bubble might then be misaligned with respect to its vacuum orientation. The DCC subsequently decays toward ordinary vacuum by radiation of soft coherent pions. The original picture of the DCC is that of a classical pion field oscillating coherently in a well defined direction in isospin space [4] and indeed, Blaizot and Krzywicki showed that such field configurations can develop with

---

<sup>1</sup>Laboratoire associé au Centre National de la Recherche Scientifique - URA00063.

suitable initial conditions [5]. This phenomenological picture leads in particular to a very simple, but very striking prediction: the  $1/\sqrt{f}$  event-by-event distribution of the neutral fraction  $f$  of radiated pions.

The idea received a boost in 1993 when Rajagopal and Wilczek proposed a microscopic mechanism for the formation of a classical coherent pion field inside the bubble [6], the so-called quench scenario: the rapid expansion causes the system, initially thermalised above the critical temperature, to cool down very rapidly, leading to the amplification of the soft pion modes via the mechanism of spinodal instability. Since then, this scenario has attracted much attention and has been further developed. In particular, quantum effects in the mean field approximation have been included (see e.g. [7, 8]) and the drastic quench approximation has been abandoned in favour of one taking the expansion explicitly into account [8, 9].

The quench scenario has been widely accepted as a microscopic description of DCC formation in heavy ion collisions and some works were dedicated to the study of its phenomenological implications [10, 11, 12]. However it is less clear than usually believed whether the typical field configuration emerging from a quenched thermal ensemble is identical to what one had in mind in the early '90s. Indeed the DCC configuration can be characterised by three essential features [1, 4, 5]:

- (a) it is a coherent field excitation, essentially a classical field configuration,
- (b) each Fourier component of the field oscillates along a well defined orientation in isospin space<sup>2</sup>,
- (c) the orientations of different modes are aligned along one single direction.

The object of the present paper is to perform a detailed statistical analysis of the generic field configuration emerging from the quench scenario in order to determine whether it exhibits a DCC structure.

For this purpose one has to choose a reliable framework. Quantum effects are not of first importance as the system is essentially classical [1]. Moreover these corrections can, so far, only be included in a mean field approximation, not suitable to study the correlations between modes. Finally, in a realistic scenario, where the quench is due to a rapid expansion, the system enters only rarely in the instability region [13]. Then, to keep the argument simple, it is worth going back to the original framework of Rajagopal and Wilczek in which the system, initially in a high temperature ( $T > T_c$ ) configuration is evolved with the full, non-linear, zero temperature equations of the classical linear  $\sigma$ -model.

---

<sup>2</sup>In the following we refer to the trajectory of one Fourier mode in isospin space as (iso-)polarisation. The case described in (b) will then be referred to as linear polarisation.

## 2 The formalism

### 2.1 The quench scenario

The chiral field is parametrized by a four-component vector field in chiral space:  $\phi = (\pi, \sigma)$  and its time evolution is governed by the classical linear  $\sigma$ -model equations of motion

$$(\partial^2 - \lambda v^2 + \lambda \phi^2(\vec{x}, t)) \phi(\vec{x}, t) = H \mathbf{n}_\sigma, \quad (1)$$

where the parameters  $v$ ,  $\lambda$  and  $H$  are related to physical quantities via:

$$m_\pi^2 = m_\sigma^2 - 2\lambda f_\pi^2 = \lambda (f_\pi^2 - v^2), \text{ and } H = f_\pi m_\pi^2,$$

and are chosen so that  $m_\pi=135$  MeV,  $m_\sigma=600$  MeV and  $f_\pi=92.5$  MeV.

The initial field configuration is sampled from a thermal ensemble at some temperature  $T > T_c$ : the values of  $\phi$  and  $\dot{\phi}$  are chosen independently on each site of the cubic lattice from gaussian distributions centered around  $\phi = \dot{\phi} = \mathbf{0}$  and with variances<sup>3</sup>  $\langle \phi_j^2 \rangle = v^2/16$  and  $\langle \dot{\phi}_j^2 \rangle = v^2/4$  ( $j = 1, 2, 3, 4$ ). The lattice spacing  $a$  has then the physical interpretation of the degenerate  $\pi$  and  $\sigma$  correlation length at temperature  $T$ ,  $a = (200 \text{ MeV})^{-1}$ .

We denote by  $\varphi(\vec{k}, t)$  and  $\dot{\varphi}(\vec{k}, t)$  the Fourier components of the field and its time derivative at time  $t$ , and choose Neumann boundary conditions so that these components are real. This is not an essential point, but it is more convenient to make this choice in discussing the question of polarization. The infrared cutoff in Fourier space is  $\Delta k = \pi/Na$  where  $Na$  is the length of the cubic box.

The important point is elsewhere: the values of  $\phi$  at distinct lattice sites are assumed to be independant gaussian random numbers. One can easily convince oneself that this implies that the values of the Fourier components  $\varphi$  and  $\dot{\varphi}$  at distinct sites of the *discretized Fourier space* are *independent* gaussian random numbers as well. In other words, there is no correlation between modes in the initial state. To create a DCC configuration, the quench mechanism has not only to be efficient in amplifying the modes (which it is), but it should also be able to *build correlations* between amplified modes.

### 2.2 Observables

Our goal is to determine whether a *generic* event in the above-described statistical ensemble looks like an ideal DCC configuration. For this purpose we shall compute the event-by-event distribution of the neutral pion fraction  $f(\vec{k})$  in

---

<sup>3</sup>In ref. [6] the variances are given for the lengths of the vectors  $\phi$  and  $\dot{\phi}$ , e.g.  $\langle \phi^2 \rangle = \sum_{j=1}^4 \langle \phi_j^2 \rangle = v^2/4$ .

the mode  $\vec{k}$  (see Eq. (6)) on the one hand, and on the other hand we shall measure the correlations of this quantity between different modes (see Eq. (11)). Let us briefly review the main ideas underlying the physics we want to describe and argue for the relevance of the above mentioned observables.

In this simplified model, although the size of the box is fixed, we have in mind a rapidly expanding system (the quench assumption is a drastic idealization of the effect of expansion). This means that after some time it becomes so dilute that the modes decouple and evolve freely. To model this we stop the evolution at some freeze-out time  $t_f$ <sup>4</sup>. The field configuration at  $t_f$  is the “initial condition” for the subsequent free evolution and determines completely the properties of the outgoing waves which describe free propagating pions. Indeed, one might consider the classical field configuration at  $t_f$  as the expectation value of the corresponding quantum field in the coherent state (we only consider the pion sector)

$$|\alpha, t_f\rangle = \exp\left(\int d^3k \, \alpha(\vec{k}, t_f) \cdot \mathbf{a}^\dagger(\vec{k})\right) |0\rangle, \quad (2)$$

with

$$\alpha \cdot \mathbf{a}^\dagger = \sum_{j=1}^3 \alpha_j a_j^\dagger,$$

where  $a_j^\dagger(\vec{k})$  is the creation operator of a free pion with isospin  $j$  and momentum  $\vec{k}$ , while  $\alpha_j(\vec{k}, t_f)$  is the eigenvalue of the corresponding annihilation operator ( $t_f$  is a parameter). The state (2) is related to the field configuration at freeze-out through ( $\omega_k = \sqrt{k^2 + m_\pi^2}$ )

$$\alpha(\vec{k}, t_f) = \frac{i\dot{\varphi}(\vec{k}, t_f) + \omega_k \varphi(\vec{k}, t_f)}{\sqrt{2\omega_k}}. \quad (3)$$

The subsequent evolution reads<sup>5</sup>

$$\alpha(\vec{k}, t > t_f) = \alpha(\vec{k}, t_f) e^{-i\omega_k(t-t_f)}. \quad (4)$$

In the following, we drop the implicit dependance on the parameter  $t_f$ , for example,  $\alpha(\vec{k})$  stands for  $\alpha(\vec{k}, t_f)$  and  $\alpha(\vec{k}, t)$  for  $\alpha(\vec{k}, t > t_f)$ . Moreover, as long as we focus our attention on one particular mode, we shall omit the

---

<sup>4</sup>A more realistic description would take into account the possible finite time extent of the freeze-out period. This would require a model for freeze-out which is out of the scope of this paper. We assume that each mode  $\vec{k}$  freezes out at  $t_f$  which can be thought as the end of a common freeze-out period.

<sup>5</sup>The “subsequent evolution” is introduced for the purpose of the argument but is not essential.

indice  $\vec{k}$ , it will be reintroduced when needed. The mean number of quanta associated with the classical wave (4) reads

$$\bar{n}_j = \langle \alpha | a_j^\dagger a_j | \alpha \rangle = |\alpha_j(t)|^2 = |\alpha_j|^2 \quad (5)$$

and is time-independent. The fraction  $f$  of neutral pions in the mode  $\vec{k}$  is

$$f = \frac{\bar{n}_3}{\bar{n}_1 + \bar{n}_2 + \bar{n}_3}. \quad (6)$$

Let us now discuss the polarisation of the outgoing waves (4). First, it is easy to see that the motion of the vector  $\boldsymbol{\varphi}^{out}(t) = \boldsymbol{\varphi}(t > t_f)$  in isospin space is planar. Indeed, the vector  $\mathbf{I} = \boldsymbol{\varphi}^{out} \times \dot{\boldsymbol{\varphi}}^{out}$  is time-independent<sup>6</sup>. The trajectory described by  $\boldsymbol{\varphi}^{out}$  is an ellipse in the plane perpendicular to  $\mathbf{I}$ . Let us call  $\mathbf{u}$  and  $L$  (resp.  $\mathbf{v}$  and  $l$ ) the direction and the half-length of the big axis (resp. of the small axis) of this ellipse ( $\mathbf{u}^2 = \mathbf{v}^2 = 1$ ,  $\mathbf{u} \cdot \mathbf{v} = 0$ ,  $\mathbf{I} = \omega l L \mathbf{u} \times \mathbf{v}$ ). One has then

$$\boldsymbol{\alpha}(t) = \sqrt{\frac{\omega}{2}} (L \mathbf{u} + i l \mathbf{v}) e^{-i(\omega(t-t_f)+\eta)}, \quad (7)$$

where  $\eta$  is some phase factor to be determined from (4). It follows that

$$\bar{n}_j = \frac{\omega}{2} (L^2 u_j^2 + l^2 v_j^2),$$

and

$$f = \frac{L^2 u_3^2 + l^2 v_3^2}{L^2 + l^2}. \quad (8)$$

We concentrate on the case of interest, namely the linear polarisation, and make explicit the  $\vec{k}$  dependance. A linearly polarised wave is characterised by the fact that  $\mathbf{I}_{\vec{k}} = \mathbf{0}$ , that is:  $l_{\vec{k}} = 0$ . Then ( $\theta_{\vec{k}}$  is the angle between  $\mathbf{u}_{\vec{k}}$  and the  $\pi_3$ -axis)

$$\begin{aligned} \boldsymbol{\alpha}_{linear}(\vec{k}, t) &= \alpha(\vec{k}) e^{-i\omega_k(t-t_f)} \mathbf{u}_{\vec{k}}, \\ f_{linear}(\vec{k}) &= \cos^2 \theta_{\vec{k}}. \end{aligned} \quad (9)$$

Because both the dynamics (Eq. (1)) and the initial ensemble are invariants under isospin rotations, there is no privileged direction in isospin space, so if such a linearly polarised wave is generically produced, the event-by-event distribution of  $f(\vec{k})$  will be given by the famous  $1/\sqrt{f}$  law. This will remain

---

<sup>6</sup> $\mathbf{I}_{\vec{k}}$  is the  $\vec{k}$  component of the conserved isorotation generators  $\int d^3x \boldsymbol{\phi}(\vec{x}, t) \times \dot{\boldsymbol{\phi}}(\vec{x}, t) = \int d^3k \boldsymbol{\varphi}(\vec{k}, t) \times \dot{\boldsymbol{\varphi}}(\vec{k}, t)$ . For  $t > t_f$  the modes are decoupled so each  $\mathbf{I}_{\vec{k}}$  is conserved.

approximately true for the more realistic case of “flat” elliptic waves ( $l_{\vec{k}} \ll L_{\vec{k}}$ ), but not otherwise<sup>7</sup>. The event-by-event distribution of the neutral fraction in one mode  $f(\vec{k})$  is then a useful observable and gives a non trivial information about the polarisation of the generic outgoing waves  $\varphi_{\vec{k}}^{out}$ .

As emphasized in the introduction, in an ideal DCC all  $\varphi_{\vec{k}}^{out}$ ’s oscillate in the same direction  $\mathbf{u}$ <sup>8</sup>

$$\boldsymbol{\alpha}_{DCC}(\vec{k}, t) = \alpha(\vec{k}) e^{-i\omega_k(t-t_f)} \mathbf{u}.$$

So, defining the total neutral pion fraction as

$$f^{tot} = \frac{N_3}{N_1 + N_2 + N_3}, \quad (10)$$

where  $N_j = \int d^3k \bar{n}_j(\vec{k})$ , one has

$$f_{DCC}^{tot} = \cos^2 \theta,$$

where  $\theta$  is the angle between  $\mathbf{u}$  and the  $\pi_3$ -axis.

For an ideal DCC, the *total* neutral pion fraction is distributed according to the  $1/\sqrt{f}$  law. In a realistic situation, only those modes undergoing amplification should be taken into account. Moreover the individual waves are neither strictly linearly polarised nor strictly aligned with each others, so one would expect some deviation from the  $1/\sqrt{f}$  law in the distribution of the total neutral pion fraction  $f^{tot}$  (see e.g. [9, 11]). We will come back to this later. In the present work, we compute the following normalized correlation function

$$C(\vec{k}, \vec{k}') = \frac{\langle f(\vec{k}) f(\vec{k}') \rangle_c}{\sqrt{\langle f^2(\vec{k}) \rangle_c \langle f^2(\vec{k}') \rangle_c}}, \quad (11)$$

where  $\langle AB \rangle_c = \langle AB \rangle - \langle A \rangle \langle B \rangle$  and  $\langle \dots \rangle$  denotes the average over the ensemble at time  $t_f$ . In the case of linearly polarised individual waves  $\varphi_{\vec{k}}^{out}$ , the  $f(\vec{k})$ ’s measure the directions of polarisation (Eq (9)) and  $C(\vec{k}, \vec{k}')$  is a measure of the degree of alignment of these directions.

---

<sup>7</sup>It is worth noting that, although it is always possible to write  $f(\vec{k})$  as the squared cosine of some angle  $\chi_{\vec{k}}$ , this angle has not, in general, the meaning of a uniform orientation in isospin space so  $f(\vec{k})$  does not, in general, follow the  $1/\sqrt{f}$  law (see Appendix). In Ref. [9], the author has a  $1/\sqrt{f}$  distribution for  $f(\vec{k} = \vec{0})$ , this comes from the fact that the time derivative of the field was not included in the definition of the particle number.

<sup>8</sup>The DCC is a zero isospin state:  $\int d^3x \mathbf{I}_{\vec{k}} = \mathbf{0}$  [4]. This is very explicitly stated in [1], but is also assumed, more or less explicitly, in all the original papers, where the DCC idea has been put forward.

### 3 Results

Our box is a  $64^3$  cubic lattice and the equations of motion (1) are implemented via a staggered leap-frog scheme [14] with time-step  $\Delta t = 0.04a$ . Once an initial condition has been chosen, one can follow the time evolution of the  $\varphi(\vec{k}, t)$ s. We reproduce completely the results of Ref. [6] with the same bin-average procedure in momentum space: in the isospin directions ( $j = 1, 2, 3$ ) the soft modes experience dramatic amplification, the softer the mode the larger the amplification, and exhibit coherent oscillations with period  $2\pi/\omega_k \sim 2\pi/m_\pi$ . Such behavior does not show up in the  $\sigma$  direction. This average behavior<sup>9</sup> can be qualitatively understood in the mean-field approximation [6, 15]: for short times  $t \lesssim 10a$ , the curvature of the effective potential (effective mass squared) is negative and the softest modes, for which the associated effective frequency is imaginary, experience amplification: this is the spinodal instability; for times  $t \gtrsim 10a$ , although this phenomenon is no more efficient (the effective mass squared is positive), the field is still significantly amplified. This is due to the mechanism of parametric resonance triggered by the regular oscillations of the mean-field around its asymptotic (vacuum) value [15, 16]. Obviously, the amplification does not grow forever and at late times ( $t \gtrsim 100a$ ) the energy is equally dissipated among the modes. In the following we present results for two values of the freeze-out time:  $t_f = 10a$  ( $21 \times 10^3$  MC events), corresponding to the end of the spinodal period, and  $t_f = 56a$  ( $10.9 \times 10^3$  MC events), which is the time when the averaged amplification of the soft modes (eq. (12)) is maximal. For simplicity we only sketch results for  $\vec{k} \equiv (k = n\Delta k, 0, 0)$ , where  $\Delta k = \pi/Na \approx 10$  MeV ( $N = 64$  is the size of the box). Moreover, the linear  $\sigma$ -model being an effective theory for energy scales  $\lesssim 100$  MeV, we only consider the window  $0 < n < 15$ .

The amplification factor in the mode  $k$  at time  $t_f$  is defined as

$$\mathcal{A}(k, t_f) = \frac{P(k, t_f)}{P(k, 0)}, \quad (12)$$

where

$$P(k, t_f) = \omega_k \sum_{j=1}^3 \bar{n}_j(k, t_f)$$

is the power spectrum in the mode  $k$  at freeze-out. The mean numbers  $\bar{n}_j(k, t_f)$  are extracted from the field configuration at time  $t$  with the help of Eqs. (3)

---

<sup>9</sup>The amplification of a particular mode exhibits large fluctuations around its average value over the ensemble. In particular it is not a smooth decreasing function of  $\|\vec{k}\|$  as revealed by an event-by-event analysis. In this respect, the binning procedure of Ref. [6] produces the same result as the ensemble average. The same is observed for the coherent behavior of the soft modes.

and (5). The  $k$ -dependance of the ensemble average amplification  $\langle \mathcal{A}(k, t_f) \rangle$  is shown in Fig. 1. It exhibits the expected shape: low momenta are amplified with respect to larger ones. Note the semi-quantitative agreement with mean-field argument for  $t_f = 10a$ : from the mechanism of spinodal instability one expects a monotonic enhancement of the modes with momenta  $k \lesssim f_\pi$ . At  $t_f = 56a$  the softest modes have grown further and the window of amplified modes has shrunk considerably.

Event-by-event distributions of the neutral fraction in different modes are shown for  $t_f = 10a$  and  $t_f = 56a$  in Figs. 3 and 4 respectively. All show large fluctuations around the mean-value  $\langle f \rangle = 1/3$ . The most amplified modes, those which we are interested in, exhibit a very different shape from the less amplified ones. A closer analysis reveals that the  $f$ -distributions of amplified modes are almost the same as in the initial ensemble (see (A.5)), whereas those of less amplified modes look very different and all follow the same linear behavior. It is interesting to note that this linear law is what is found in a thermal ensemble of pions (see (A.8)), supporting the idea that these modes are already thermalised.

Fig. 6 gives a more precise picture of the above statements. It represents the average eccentricity<sup>10</sup> of the ellipse (7) as a function of the momentum. One sees that for  $t_f = 10a$  the average polarisation is close to its initial value for almost the whole studied range of momenta, whereas for  $t_f = 56a$  only the few first modes remain close to their initial value, the average eccentricity being constant for  $k \gtrsim 50$  MeV. Note the correlation between the shapes of the average amplification and of the average eccentricity as functions of  $k$ . Note also that, although the eccentricity of the softest modes decreases as these modes are amplified, this is a very tiny effect<sup>11</sup> and in fact the shapes of their neutral fraction distribution at freeze-out time are mostly determined by the corresponding initial distributions.

So we see that the modes are far from being strictly linearly polarised waves, but this causes only a small deviation from the ideal  $1/\sqrt{f}$  law. There are still important event-by-event fluctuations of the neutral fraction of pions with momentum  $k$ , so that from the point of view of an experimentalist the deviation is not very important.

Finally, Fig. 7 shows the correlation function (11): at both freeze out times the different modes remain completely uncorrelated. In terms of the average coherent behavior described at the beginning of this section, this means that although the vectors  $\varphi_{\vec{k}}$  corresponding to amplified modes do oscillate co-

<sup>10</sup>The eccentricity of an ellipse is defined as the ratio of the lengths of its small to its big axes, i.e., in the notations of (7),  $e_k = l_k/L_k$ .

<sup>11</sup>An event-by-event analysis shows that the proportion of events in which the zero-mode eccentricity is lower than 0.1 is: 13% in the initial state, 16% at  $t_f = 10a$  and 18% at  $t_f = 56a$ .



herently, their mean directions of oscillation in isospin space (say, the directions of their big axes) are completely random: different modes act as independent DCCs. The obvious phenomenological consequence is that the signal is washed out when summing up the contributions of different momenta as in Eq (10). This is illustrated in Fig. 5 where we show the distributions coming from the contribution of five and ten equivalent modes (that is modes having almost the same individual neutral fraction distributions).

## 4 Discussion

### 4.1 Summary

Starting from a chirally symmetric thermal ensemble for the field  $\phi \equiv (\pi, \sigma)$ , we evolved the system with the zero temperature equation of motion of the linear  $\sigma$ -model. This quenching of initial (thermal) fluctuations is a very efficient mechanism for producing large and coherent long wavelength oscillations of the pion field at intermediate times [6].

We performed a detailed analysis of the emerging field configuration which shows that nothing significant happens concerning its isospin structure. The neutral fraction distribution of the amplified, long wavelength modes is essentially the same as it was in the initial ensemble. Although not exactly  $1/\sqrt{f}$ , the distribution is very broad, which is a relevant point for phenomenology. However, we found that distinct modes, and in particular the amplified ones, have completely independent polarisations in isospin space. This has the important phenomenological consequence: the large event-by-event fluctuations of the neutral fraction are washed out when the contributions of several modes are added, even when one limits one's attention to soft modes only.

The key point is to realise that the assumption of a completely randomized initial state made in Ref. [6] implies that, in the initial configuration, the field modes are also independent gaussian random numbers. So our result can be rephrased as follows: the non-linearity of the dynamics does *not* build correlations between modes. The initially postulated chaos is recovered in the final state. This contradicts the widely made assumption that the state produced in the simplest form of the quench scenario (initially thermalized system) is identical to the originally proposed DCC. The quenching explains the emergence of a strong, coherent pion field, not its hypothetical polarization.

### 4.2 Comparison with other works

Analogous results to that shown in Fig. 5 were obtained before by several authors [10, 11, 12]. We briefly review them below.

Gavin, Gocksch and Pisarski argue in [10] that the system is composed of “many small, randomly-oriented domains” resulting in a binomial distribution of the neutral fraction of the *total* number of pions. However, as was pointed out later by Rajagopal [2], the system cannot be characterised by a single length scale and the picture of different domains of the size of the correlation length is not adequate. In the present paper we have shown indeed that the typical field configuration emerging from the quench scenario is a superposition of misaligned waves in momentum space: different *modes* and not different domains act as independant DCCs<sup>12</sup>.

In Ref. [11], Rajagopal had in mind a disoriented condensate formed by the amplified, long wavelength modes “superposed with short wavelength noise”. After binning phase space, he computes the bin-by-bin distribution of the neutral fraction of pions with  $\|\vec{k}\| \lesssim 300$  MeV and observes “an admixture of a  $1/\sqrt{f}$  distribution”. This momentum space picture is more satisfactory. Indeed the observation that modes of different types (amplified vs. thermalized) contribute incoherently and delay the signal is in line with our present result. However, we saw that soft modes do not act together to form a coherent misaligned condensate, their polarizations are uncorrelated.

Finally, Randrup, studying DCC observables in [12], computes the distribution of the neutral fraction of pions with momenta below different cutoffs. From this he argues that “each  $\vec{k}$  contributes pions having an independant orientation in isospace”. This is exactly what we have found here. However, Randrup’s analysis is performed in a model with expansion. This means that not all the events entering the analysis have experienced amplification. In this sense his work is incomplete and therefore not really conclusive on the matter we are interested in here.

Hence, some of the features of the quench scenario have been noticed in earlier studies. However, nobody has carried out a detailed statistical analysis of the correlation between mode polarizations. In this respect, we believe, our work helps to clarify the situation.

### 4.3 Speculations

As already mentioned, the simplest form of the quench scenario is not sufficient to produce a DCC configuration. Inclusion of quantum effects at the mean-field level or of expansion will probably not change this. Instead, it would be instructive to refine the description by including correlations in the initial state.

---

<sup>12</sup>This does not exclude the possibility a priori that many such domains form in heavy ion collisions. However, we argued, in a recent work with A. Krzywicki, that the formation of many bubbles undergoing strong amplification is not likely [13].

A possible way of including initial correlations could be to relax the thermal approximation for soft modes. Indeed, if the quench mechanism appears to be quite natural in the context of high energy heavy ion collisions, it is not clear whether the assumption that the initial system is fully thermalized is justified. In particular, in such small systems, long wavelength modes may not have enough time to thermalize, as it is the case in [6] (see also Fig.1). Correlations in the initial state could possibly be amplified by the subsequent out of equilibrium evolution. Indeed, from mean-field arguments, the spinodal amplification is expected to be quite robust against a large class of initial conditions<sup>13</sup>. One has then to have a reliable model for the initial state, that is a model for the early stages of the collision.

Finally, if some correlations are present in a realistic description of our initial state, it could be that they do not survive the non-linear dynamics. One would be left again with an incoherent superposition of disoriented waves in the final state. In such a situation, large fluctuations of the neutral fraction of pions in a bin of phase space would only be detectable if one can separate individual modes as well as possible. The volume of the bubble should be large enough to have a good statistics in each bin, and small enough to have as few as possible modes in each bin.

## 4.4 Conclusion

We believe that a complete microscopic understanding of DCC formation in heavy ion collisions is not achieved yet. It might also be, however, that the original picture of DCC is a too far going idealization. Future investigations will tell whether it is the original picture or the quench scenario which has to be modified. Theoretical developpements as well as experimental data are called for.

## Acknowledgment

I am very grateful to A. Krzywicki, J.P. Blaizot, and M. Joyce for useful conversations and comments and for careful reading of the manuscript.

---

<sup>13</sup>The main restriction being that initial fluctuations should not be too large in order to enter the instability region (negative effective mass squared).

## A Appendix: neutral fraction distribution in a gaussian model

It is instructive to compute the distribution of the neutral fraction  $f$  for the following class of statistical ensembles: let us consider the  $\varphi_{\vec{k}}$ 's and the  $\dot{\varphi}_{\vec{k}}$ 's as independant gaussian numbers with zero mean value and dispersions  $a$  and  $b$  respectively ( $a$  and  $b$  are the same for each mode and for each isospin direction). We write the probability ( $c$  stands for  $\{j, \vec{k}\}$ )

$$Proba(\{\varphi_{\vec{k}}\}, \{\dot{\varphi}_{\vec{k}}\}) = \prod_c P_{\varphi}(\varphi_c) P_{\dot{\varphi}}(\dot{\varphi}_c) d\varphi_c d\dot{\varphi}_c, \quad (\text{A.1})$$

$$\begin{aligned} P_{\varphi}(x) &= \frac{1}{\sqrt{2\pi a^2}} \exp\left(-\frac{x^2}{2a^2}\right), \\ P_{\dot{\varphi}}(x) &= \frac{1}{\sqrt{2\pi b^2}} \exp\left(-\frac{x^2}{2b^2}\right). \end{aligned} \quad (\text{A.2})$$

The modes being independant, we focus on one particular  $\vec{k}$  and drop the indice. From Eq. (3) we have for each isospin component

$$\begin{aligned} \varphi &= \sqrt{\frac{2}{\omega}} \text{Re}\alpha = A \cos \gamma, \\ \dot{\varphi} &= \sqrt{2\omega} \text{Im}\alpha = \omega A \sin \gamma, \end{aligned} \quad (\text{A.3})$$

where  $\gamma$  is defined through  $\alpha = \sqrt{n} e^{i\gamma}$ , and  $A = \sqrt{2n/\omega}$ . The probability distribution for the amplitude  $A$  and the angle  $\gamma$  is given by

$$P_{A,\gamma}(A, \gamma) = \omega A P_{\varphi}(A \cos \gamma) P_{\dot{\varphi}}(\omega A \sin \gamma). \quad (\text{A.4})$$

The probability distribution of the neutral fraction  $f = A_3^2/(A_1^2 + A_2^2 + A_3^2)$  is

$$P_f(f) = \int_0^{+\infty} dx dy dz P_A(x) P_A(y) P_A(z) \delta\left(f - \frac{z^2}{x^2 + y^2 + z^2}\right),$$

where

$$P_A(A) = \int_0^{2\pi} d\gamma P_{A,\gamma}(A, \gamma).$$

After some calculations one gets

$$P_f(f) = \frac{1}{2} (F_{\Omega}(f) + F_{-\Omega}(f)), \quad (\text{A.5})$$

where

$$F_{\Omega}(f) = (\Omega - (1 - f)) \left( \frac{\Omega + 1}{\Omega - (1 - 2f)} \right)^{3/2},$$

and

$$\Omega = \frac{b^2 + \omega a^2}{b^2 - \omega a^2}.$$

It is instructive to look at some specific examples of (A.2). First, we can fix one of the two vectors  $\varphi$  and  $\dot{\varphi}$  to be zero. In this case  $\alpha$  is proportional to a randomly oriented vector in isospin space and one recovers the  $1/\sqrt{f}$  law. Indeed, let us choose  $b = 0$  ( $\Omega = -1$ ), that is  $\dot{\varphi} = \mathbf{0}$ . Then  $\alpha \sim \varphi$  and

$$P_f(f) = \frac{1}{2\sqrt{f}}. \quad (\text{A.6})$$

The second interesting example is the case where  $b = \omega a$  ( $\Omega = +\infty$ ). In terms of a probability distribution for the complex numbers  $\alpha_j = x_j + iy_j$ <sup>14</sup>

$$P_\alpha(\alpha) d^2\alpha = P_{x,y}(x, y) dx dy,$$

one has, from (A.2) and (A.3),

$$P_\alpha(\alpha) = \frac{1}{\pi\sigma^2} e^{-|\alpha|^2/\sigma^2}, \quad (\text{A.7})$$

where

$$\sigma^2 = a b = \langle \bar{n} \rangle = \int d^2\alpha P_\alpha(\alpha) |\alpha|^2$$

( $|\alpha|^2 = \bar{n}$  is the mean number of quanta in the coherent state  $|\alpha\rangle$  and  $\langle \bar{n} \rangle$  in the mean number of quanta in the statistical ensemble).

For the class of ensembles (A.7), the neutral fraction distribution reads

$$P_f(f) = 2(1 - f). \quad (\text{A.8})$$

A particular case of (A.7) is that of a thermal collection of quanta with frequencies  $\omega$ .

Finally, the initial ensemble used in the quench scenario belongs to the class (A.1). The  $\phi_j(\vec{x})$ 's and the  $\dot{\phi}_j(\vec{x})$ 's are independant gaussian numbers of variances  $\langle \phi_j^2 \rangle$  and  $\langle \dot{\phi}_j^2 \rangle$  respectively. This implies that the  $\varphi_j(\vec{k})$ 's and the  $\dot{\varphi}_j(\vec{k})$ 's are independant gaussian numbers of variances  $\mathcal{N} \langle \phi_j^2 \rangle$  and  $\mathcal{N} \langle \dot{\phi}_j^2 \rangle$  respectively ( $\mathcal{N}$  is a normalisation factor)

$$a^2 = \mathcal{N} \langle \phi_j^2 \rangle = \mathcal{N} \frac{v^2}{16}, \quad b^2 = \mathcal{N} \langle \dot{\phi}_j^2 \rangle = \mathcal{N} \frac{v^2}{4},$$

and

$$\Omega = \frac{4 + \omega^2}{4 - \omega^2}.$$

Fig. 2 shows the neutral fraction distribution in the initial ensemble for the two extremal values of the studied window  $0 \leq k \lesssim 150 \text{ MeV}$ <sup>15</sup>.

---

<sup>14</sup>Such a probability distribution for the  $\alpha$ 's is called the P-representation of the density operator [17]: a very large class of quantum density operators can be written  $\hat{\rho} = \int d^2\alpha P_\alpha(\alpha) |\alpha\rangle \langle \alpha|$ .

<sup>15</sup>Note that although our initial state is a thermal collection of quanta, these are not zero

## References

- [1] G. Amelino-Camelia, J.D. Bjorken, S.E. Larsson Phys. Rev. D56 (1997) 6942.
- [2] K. Rajagopal, in *Quark-Gluon Plasma 2*, ed. R. Hwa, World Scientific, 1995.;  
J.P. Blaizot and A. Krzywicki, Acta Phys. Polon. 27 (1996) 1687.
- [3] The Minimax Collaboration, Phys. Rev. D61 (2000) 032003; The WA98 Collaboration, Nucl. Phys. A638 (1998) 249c.
- [4] J.D. Bjorken, Int. J. Mod. Phys. A7 (1992) 4189; Acta Phys. Polon. B23 (1992) 637.
- [5] J.P. Blaizot and A. Krzywicki, Phys. Rev. D46 (1992) 246; Phys. Rev. D50 (1994) 442.
- [6] K. Rajagopal and F. Wilczek, Nucl. Phys. B399 (1993) 395; Nucl. Phys. B404 (1993) 577.
- [7] D. Boyanovsky, H.J. de Vega, R. Holman Phys. Rev. D51 (1995) 734.
- [8] F. Cooper, Y. Kluger, E. Mottola, J.P. Paz, Phys. Rev. D51 (1995) 2377;  
M.A. Lampert, J.F. Dawson, F. Cooper, Phys. Rev. D54 (1996) 2213.
- [9] J. Randrup, Phys. Rev. Lett. 77 (1996) 1226.
- [10] S. Gavin, A. Gocksch, R.D. Pisarski Phys. Rev. Lett. 72 (1994) 2143.
- [11] K. Rajagopal, hep-ph/9703258
- [12] J. Randrup, Nucl. Phys. A616 (1997) 531.
- [13] A. Krzywicki and J. Serreau, Phys. Lett, B448 (1999) 257.
- [14] Numerical Recipes, ed. Cambridge University Press.
- [15] D. Kaiser, Phys. Rev. D59 (1999) 117901.
- [16] A. Dumitru and O. Scavenius, hep-ph/0003134.
- [17] R.J. Glauber, Phys. Rev. 131 (1963) 2766.

---

temperature pions (this means that their dispersion relations are not those of free pions). That is why the initial neutral fraction distribution is not the same as (A.8).

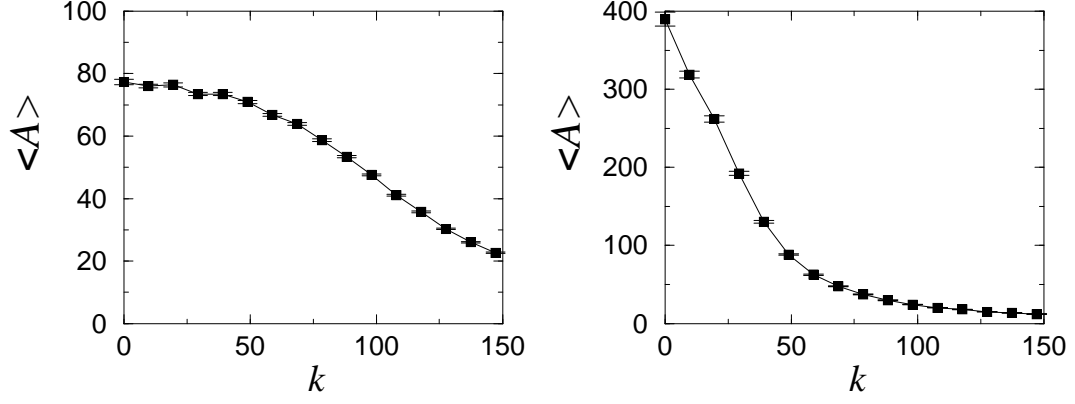


Figure 1: The average amplification  $\langle \mathcal{A}(k, t_f) \rangle$  as a function of  $k$  (MeV) for  $t_f = 10a$  (left) and  $t_f = 56a$  (right). The error bars represent statistical errors and the lines are just guides for the eyes.

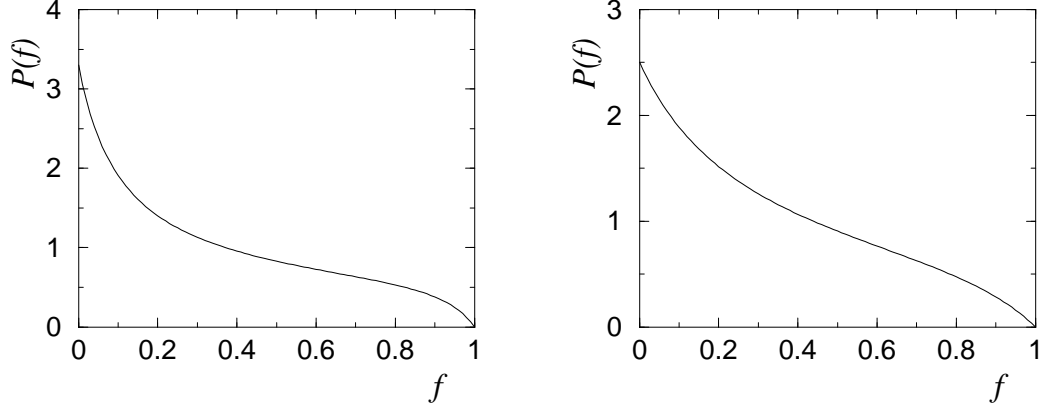


Figure 2: Neutral fraction distribution in the initial ensemble for  $n = 0$  (left) and  $n = 15$  (right).

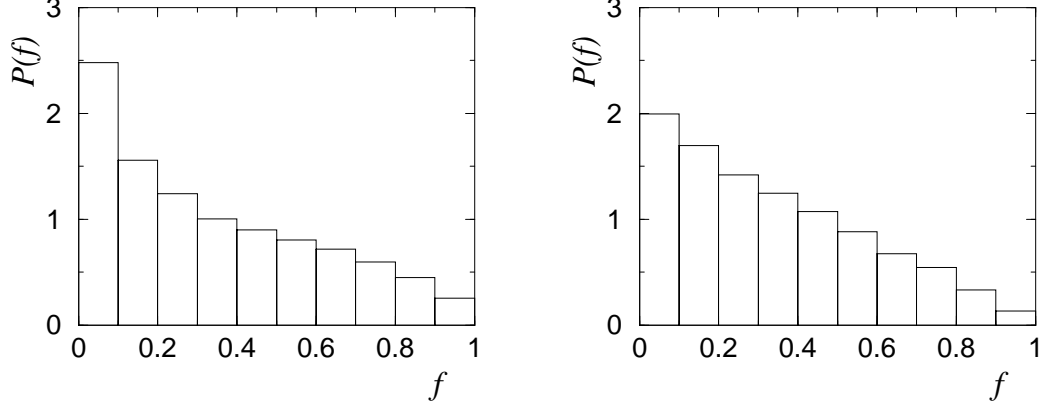


Figure 3: Neutral fraction distributions at time  $t_f = 10a$  for  $n = 0$  (left) and  $n = 15$  (right) ( $k = n\Delta k$  with  $\Delta k \simeq 10$  MeV). All the histograms for  $n \leq 14$  are compatible with the corresponding initial distributions while  $n = 15$  already exhibit a linear shape to be compared with the  $2(1-f)$  neutral fraction distribution in a thermal ensemble (Eq. (A.8)).

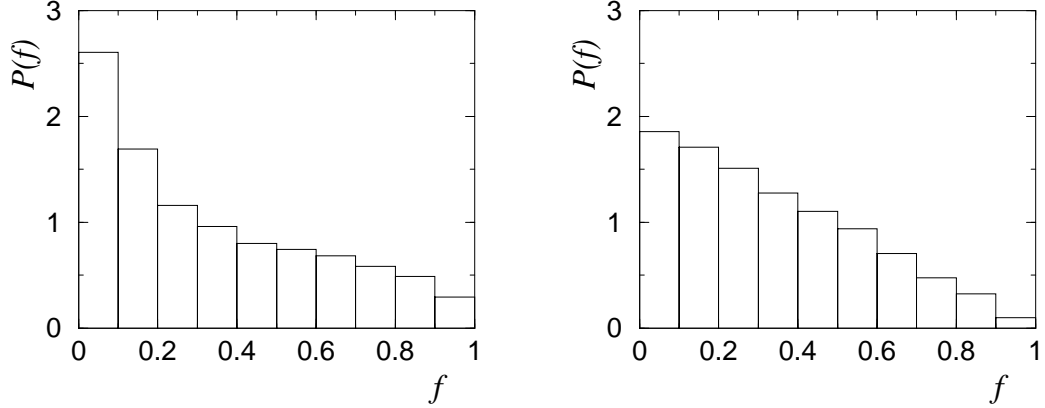


Figure 4: Neutral fraction distributions at time  $t_f = 56a$  for  $n = 0$  (left) and  $n = 4$  (right) ( $k = n\Delta k$  with  $\Delta k \simeq 10$  MeV). The histograms for  $n \leq 3$  follow the corresponding initial distributions. All the modes  $n \geq 4$  exhibit the same linear shape.



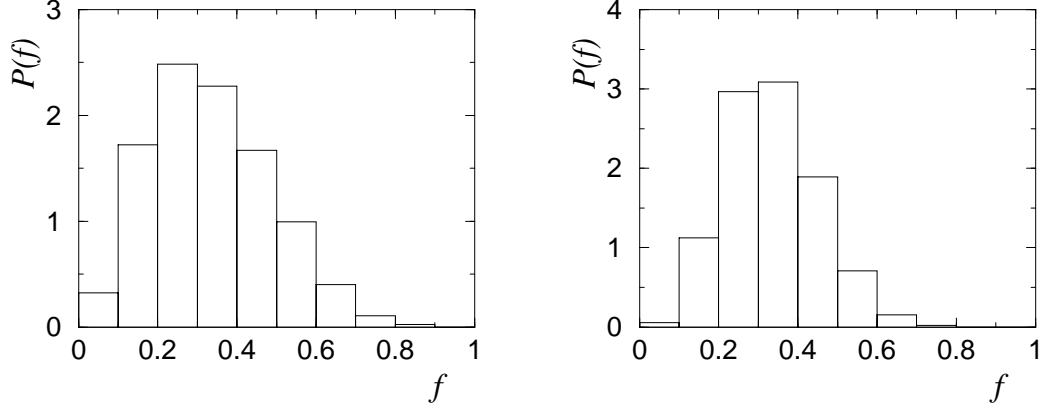


Figure 5: Neutral fraction distributions where we took into account the contributions of modes with  $n = 0, \dots, 4$  (left) and  $n = 0, \dots, 10$  (right) at  $t_f = 10a$ . At this time all these modes have essentially the same individual distribution (cf. Fig. 3).

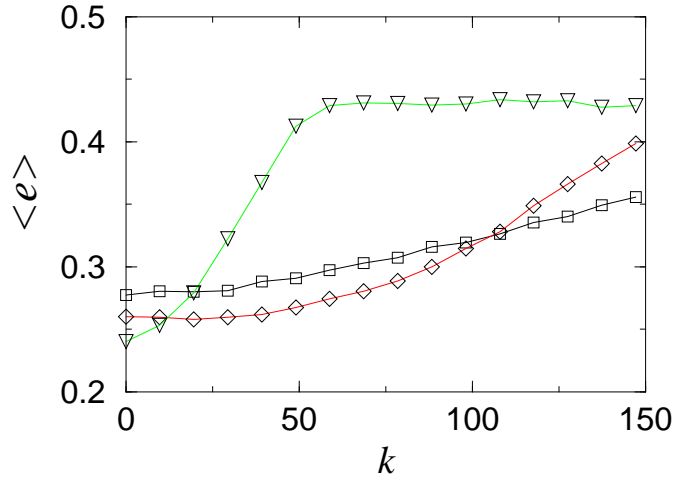


Figure 6: The average excentricity  $\langle e(k, t_f) \rangle$  as a function of  $k$  (MeV) in the initial ensemble (square) and for  $t_f = 10a$  (diamond) and  $t_f = 56a$  (triangle). The lines are just guides for the eyes.

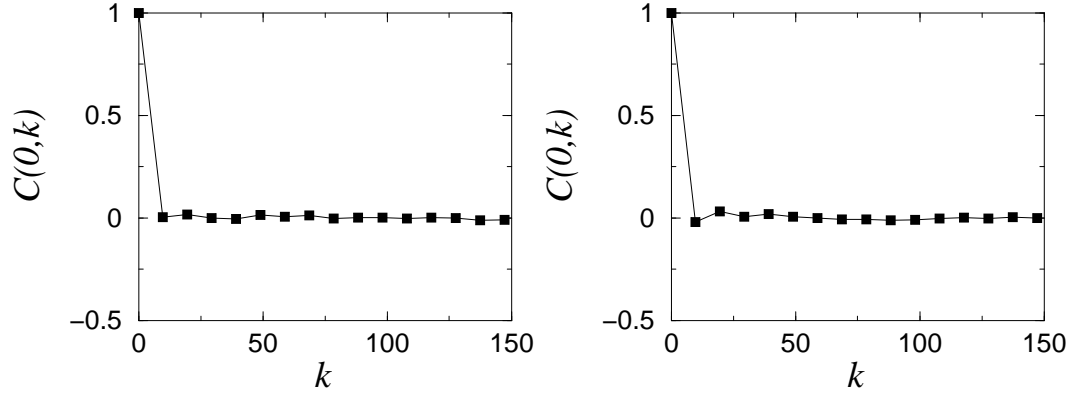


Figure 7: The correlation function  $C(0, k)$  (Eq. (11)) vs.  $k$  (MeV) for  $t_f = 5a$  (left) and  $t_f = 56a$  (right). We computed also  $C(k_0, k)$  as a function of  $k$  for different values of  $k_0$ , all look the same as above.